Kaplan turbine working as a propeller: CFD investigation and experimental validation of generated power fluctuation

IOP Conf. Series: Earth and Environmental Science **240** (2019) 022049 doi:10.1088/1755-1315/240/2/022049

Kaplan turbine working as a propeller: CFD investigation and experimental validation of generated power fluctuation

M Angulo, A Rivetti, C Lucino and S Liscia

Laboratory of Hydromechanics, UNLP, 47 street Nº 200, 1900 La Plata, Argentina

E-mail: mauriangulo@gmail.com

Abstract. Thanks to their ability to adjust automatically the guide vane and runner blades position, the use of Kaplan turbines is advantageous compared to other types in terms of power regulation, as a high efficiency can be attained over a wide range of head and power. However, such features have a cost of a more complex design of the components inside the hub and the main shaft. The number of daily movements of all these components, which is linked to the required power and frequency regulation, leads to wearing and fatigue in the long term. Therefore, the replacement and reparation of components are regular maintenance tasks which, on some occasions, might entail the dismantling of the turbine and the generator when some key hub components fails. In the face of such events, a cost-benefit-based decision must be made concerning to whether repair the turbine to recover its functionality or to operate the Kaplan turbine in propeller mode. In propeller mode, the turbine can operate at on-cam condition for a single load for any given head. For loads other than the corresponding to on-cam condition, an acceptable hydraulic behaviour is not guaranteed, since such use is usually not contemplated in acceptance tests. Therefore, pressure fluctuation due to vortex rope development, cavitation, power instability and structural vibration may arise at loads other than the corresponding to on cam operation. One of the main issues that limits the operation range is the generated power oscillation due to partial load vortex development. This paper presents numerical investigations focusing in this phenomenon. The computational domain includes guide vanes, runner and draft tube. Also, a simplified draft tube consisting in a symmetrical revolution volume is explored. Measurements were performed at prototype scale at same operating conditions and pressure fluctuations, power generation, vibrations and sound emission were recorded. These measurements are then shown and compared with CFD results.

1. Introduction

Kaplan turbines have a great advantage compared to other types in terms of power regulation. This advantage is held on the capability to adjust automatically the guide vane and runner blades positions, providing the capacity to hold high efficiency over a wide range of head and power. This feature leads to higher construction costs and more complex design of the components inside the hub and the main shaft.

The internal mechanism that allows the rotation of the blades while the runner is spinning consist of several components. Despite there are many different designs, there are common parts such as: the Kaplan oil head, the oil supply pipes, and the internal mechanism of the hub.

Depending on the power grid requirements, power and frequency regulation, the Kaplan mechanism has several daily movements that cumulated along years produce wearing and fatigue, so the need to replace a component is a regular maintenance task. Most of the components are accessible to be repaired or replaced. The Kaplan head and pipes can be completely disassembled to repair tasks, but for some hub components it is necessary to dissemble completely the turbine and generator outside of the turbine pit.

This situation may seem an extraordinary fact, but it is not. Just to mention a few cases, five Kaplan power stations at the United States, with a total of 25 turbines, have reported the failure of the Kaplan mechanism that forced these units to operate with blocked blades [1]. This new "forced propeller operation condition" was not expected to happen, then its convenient operation zone in order to preserve the machine integrity is unknown.

Stakeholders and the technical staff at power station should decide whether to repair the turbine to recover its functionality, operate the Kaplan as a propeller or a mix of both until the repair task is possible in terms of outcomes and energy production.

Two ways of converting Kaplan to propeller are possible: to use pins that block the blade trunnion to the hub, or to use a pair of stop blocks welded to the hub at each blade. The first solution is more permanent while the second is more frequently applied in short term operation.

The next question to solve is related to the unknown "new turbine" capabilities, due to the fact that the turbine has not been tested as a propeller machine. Angulo et al [2] performed tests on physical scale of a Kaplan turbine working in propeller mode in order to define the operation zone limits and to visualize flow patterns related to partial load operation.

In this work, a different approach, based on CFD simulations, is presented. As it was previously mentioned, one of the main limiting factors when defining the operation zone is the power swing at partial load [2], among other parameters such as vibration at guide bearing and discharge ring; or pressure fluctuations at draft tube. The aim of these simulations is to capture the power fluctuation at partial load with the aim of defining the operation limits by means of CFD, avoiding physical model testing.

At the same time, measurements at prototype are shown for same operating conditions in order to test the capability of CFD simulations to capture the very beginning of the power swing. Data collected with accelerometers, sonometer, and pressure sensors are shown additionally to electrical power swing measurements.

The study introduced herein was carried out under the framework of a project focused on the dynamic behavior of Kaplan turbines that combines prototype measurements, model tests and CFD simulations.

2. Materials and methods

2.1. Prototype

Measurements on this study were performed on the turbine Kaplan unit # 3 of the binational Yacyretá power station located on the Paraná River, Argentina-Paraguay. The turbine has five blades and a 9.5 m runner. The power plant has an installed capacity of 3100 MW (20 x 155 MW) and operates on a range of heads between 19.5 m and 24.1 m, where 22.7 m in the most frequent head. The rotational velocity of the turbine is 71.42 rpm and the BEP (best efficiency point) head is 28 m. The stator has 24 guide and stay vanes. The runner blades have an anti-cavitation lip and the stainless-steel discharge ring extends 0.21 D_p downstream from the runner centerline. The runner blades have been blocked at 32.3º with a pair of stop blocks fixed to the pressure side of the blades, figure 1. Inspection and tests at prototype were performed after 11,400 hrs of operation.

Figure 1. Prototype. Two stop blocks on the pressure side of the blades to fix the opening.

2.1.1 Instrumental

Table 1 summarizes the equipment installed at the prototype and figure 2. indicates the physical position for each one.

Table 1. Prototype instrumental.

Instrument	Nomenclature	Characteristics	Prototype
Accelerometer #1	AC1	Brand	Wilcoxon Research
		Model	793L
		Position	Shaft guide bearing (radial)
		Range	+/- 10 g
		DA frequency	4,200 Hz
		Res. freq.	15 kHz
Accelerometer #2	AC2	Brand	Wilcoxon Research
		Model	793L
		Position	Discharge ring (radial)[1]
		Range	+/- 10 g
		DA frequency	4,200 Hz
		Res. freq.	15 kHz
Pressure sensor	PS	Brand	Keller
		Model	PAA-21Y
		Position	Discharge ring[1]
		DA frequency	4,200 Hz
2 Proximity sensors	PX	Brand	Bentley Nevada
		Model	7200
		Position	Over guide bearing casing
		DA frequency	100 Hz
Sonometer	SM	Brand	Bruel & Kjaer
		Model	2270 BZ-7222
		Position	Discharge ring[2]
Active Power transducer	P	Brand	Enerdis
		Model	TNE9334 PAR1232B
		Range	0-160 MW
		Precision	0.5%
		DA frequency	100 Hz
Data Acquisition system	DAS	Brand	NI
		Model	SCXI-1600 USB
		Inputs	352 analog
		Resolution	16 bits
		DA frequency	200 kS/s

[1] 0.35 Dp downstream the runner centerline
[2] At 1 m from the man door and 1 m from ground of access gallery

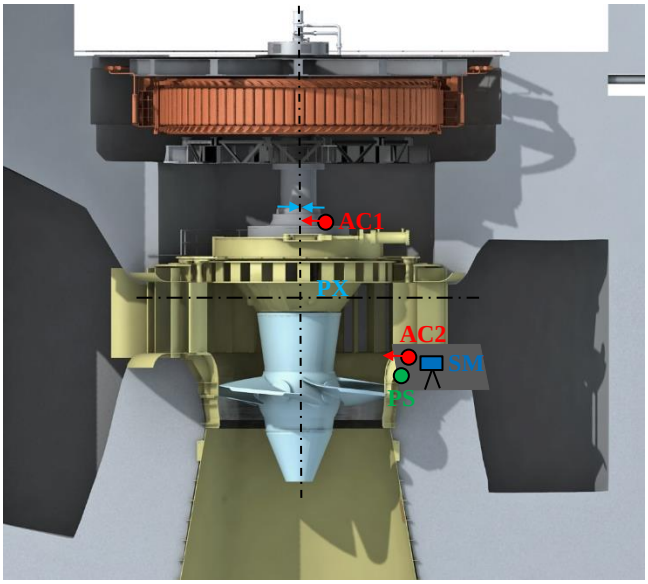

Figure 2. Prototype sensors position. Source: EBY.

2.1.2 Test procedure

The test consisted in acquiring data for every guide vane opening step of 1% below the on-cam position, denoted as Δα, where the negative sign indicates a closing direction. Ten guide vane positions were tested, starting from the on-cam opening (Δα =0). On-cam position is automatically set by the governor which depends on the actual head at the power station. For the next steps, the control of the machine is switched to manual operation mode in order to operate in off-cam mode. A 40 sec. long record was acquired for each point with a lag time between them of at least 3 min to stabilize the power output. The test was done at 0.97 of rated net head, and at sigma condition of 1.006, figure 3.

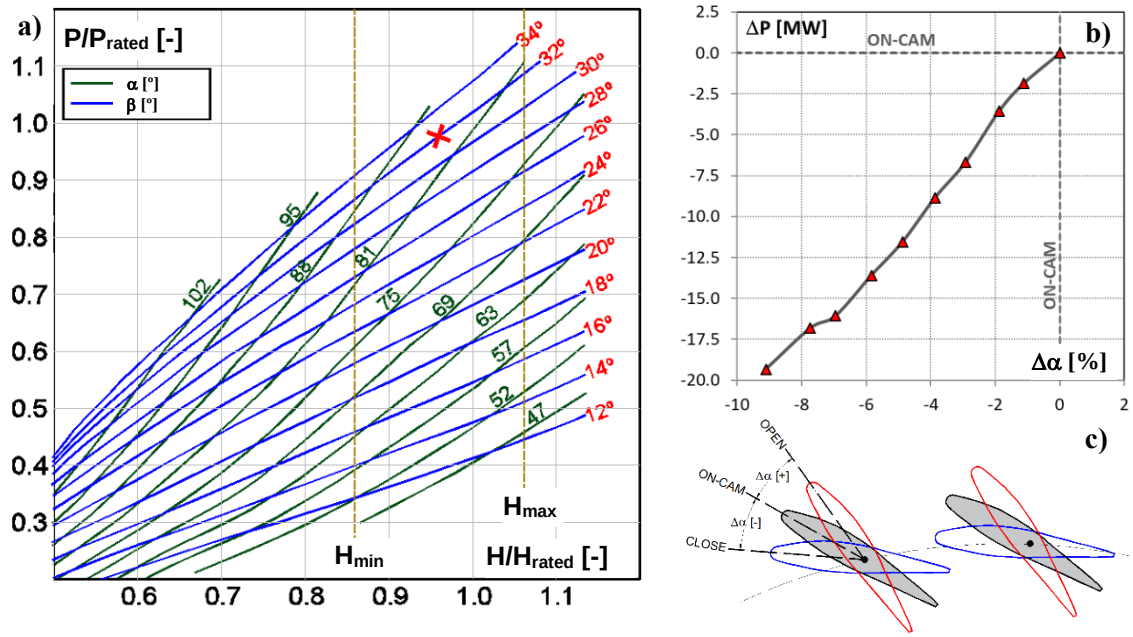

Figure 3. Kaplan turbine hill chart. a) On-cam point tested at propeller mode (Red Cross). b) Test points at propeller mode starting from the on-cam position. α: guide vane opening. β: runner blade opening. c) Reference for Δα [%], negative indicates closing direction and positive indicates opening direction.

2.2. CFD simulations

The numerical simulation is performed using the commercial code ANSYS CFX 18.0, that solves the Unsteady Reynolds Average Navier-Stokes equations (URANS). The turbulence model used to close the system of equations is the SST, and the advection scheme imposed is of the second order, both in space and time. For all the cases simulated, first a steady-state flow simulation is performed to use it as the initial flow conditions. In this case, a frozen rotor interface is used to make the stationary and rotating domains compatible. For the transient case, a transient-rotor-stator interface is used within the runner and the draft-tube domain. A time step corresponding to 5° of rotation is chosen, in order to capture the dynamic behaviour of the machine. Convergence is reached for root mean square (RMS) average of normalized velocities and pressure residuals between 10^{-5} and 10^{-6} in all cases. In table 2 the simulated points are summarized. For each case the domain and mesh for the stator is modified to represent the corresponding guide vane opening in terms of $\Delta\alpha$ [%] and the mechanical power expressed relative to the on-cam power.

Table 2. Simulated points.

Point	Δα [%]	ΔP [MW]	ΔQ [m^3/s]	C_r [m/s]	C_θ [m/s]
1	0% (ON-CAM)	0	0,0	4,55	4,55
2	-2,8	-5,9	-41,0	4,25	4,25
3	-5,3	-8	-58,0	4,21	4,21
4	-7,9	-17,5	-80,2	4,08	4,08

Boundary conditions are chosen so that they can reproduce the same operating point as that studied for prototype measurements. The operating information obtained from measurements consists in: power output, net head, tail water level and the opening of the guide vanes and runner blades. The flow rate is obtained from the hill chart and used to compute the cylindrical velocity components at the inlet section, figure 4(a).

Average static pressure is set at the outlet. The value for the pressure outlet is set to zero, and a hydrostatical reference level (Δz) is set to have the same pressure profile as prototype. A value of 1 atm is adopted as the reference pressure. The general grid interface (GGI) is used to materialize the connections between adjacent domains. The no-slip condition is imposed on all the solid surfaces and a counter-rotating wall configuration is set for the surfaces composing the rotating domain that are not rotating.

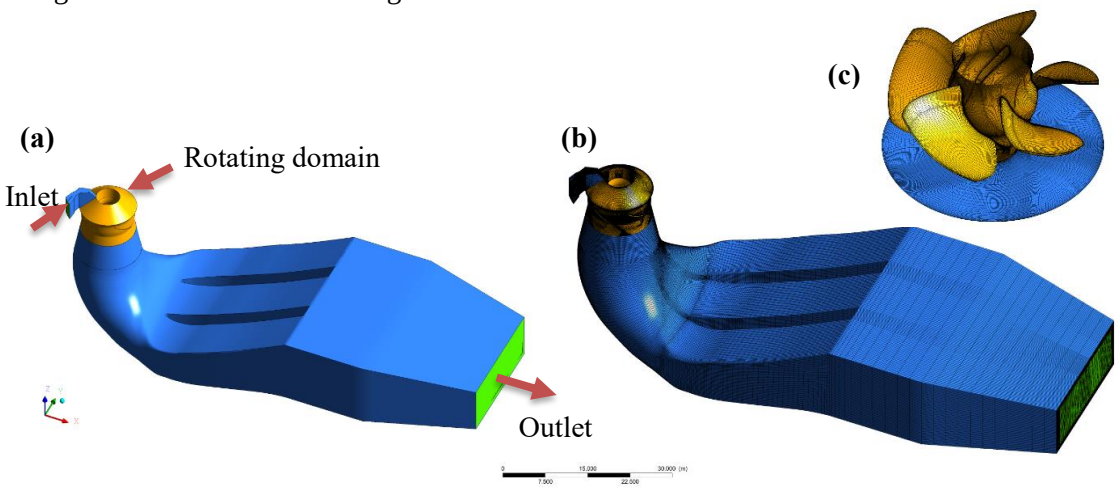

Figure 4. Computational domain showing the stationary and rotating parts (a). Hexahedral mesh used for spatial discretization (b). Mesh detail of the runner and the interface between the runner and the draft-tube (c).

3. Results

3.1 Prototype

Measurements for closing direction of the guide vanes (-Δα) where processed to visualize the global behavior of the machine at off-cam condition. This information is shown at figures 5, 6 and 7. Each graph has the same horizontal axis Δα [%]. As it can be observed vibrations at the discharge ring [figure 5.(a)], pressure fluctuations at the draft tube for the raw signal [figure 5.(b)], together with radial vibrations at the shaft guide bearing [figure 5.(a)] and sound level at the draft tube access gallery [figure 6.(a)], decrease with guide vanes closing direction. The distance between the shaft and the guide bearing casing shows a constant behaviour [figure 6.(b)]. Only power fluctuation has an increase when the distributor close, being the partial load rope the reason for this swing as it could be visualized at physical model tests [2], see figure 10.(b).

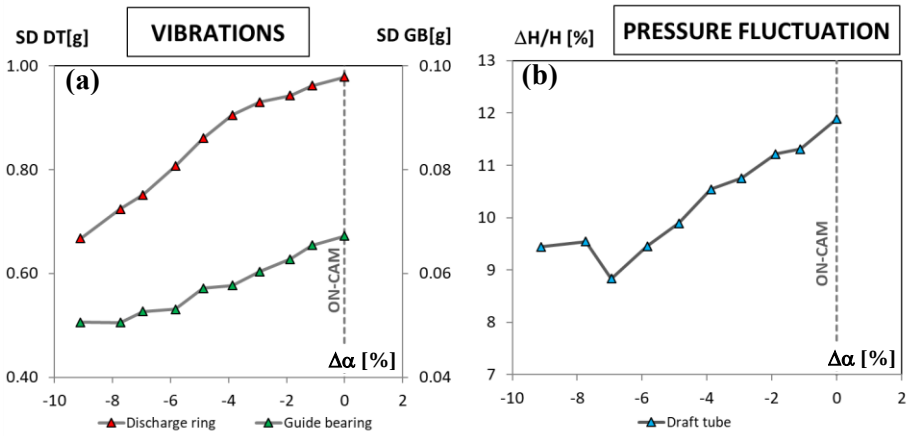

Figure 5. Standard deviation of radial vibration at the draft tube and the shaft guide bearing radial vibration (a). Pressure fluctuations at the draft tube with a 97% of confidence for the raw signal (b).

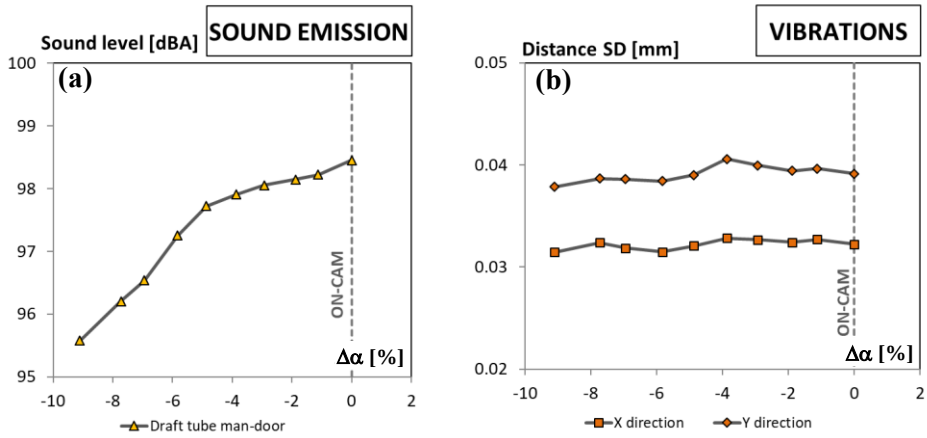

Figure 6. Average sound level in front of the draft tube man door (a). Standard deviation of the radial distance between the turbine shaft and the guide bearing casing for orthogonal directions (b).

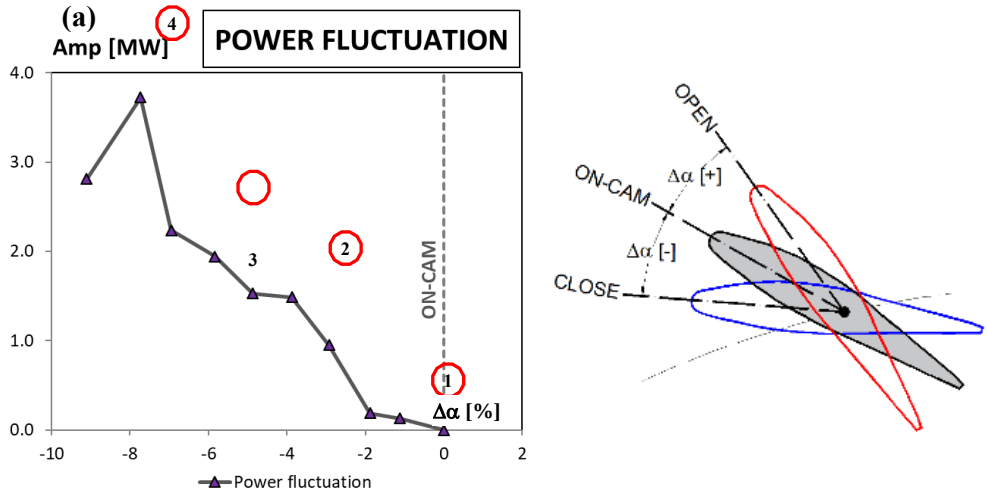

Figure 7. Amplitude of the electrical power swing signal with a confidence of 97% measured at prototype. The amplitude measured for the on-cam position is considered zero as a reference. Numbers (1 to 4) corresponds to guide vane openings simulated with CFD (a). Reference for relative guide vane opening, Δα [%] (b).

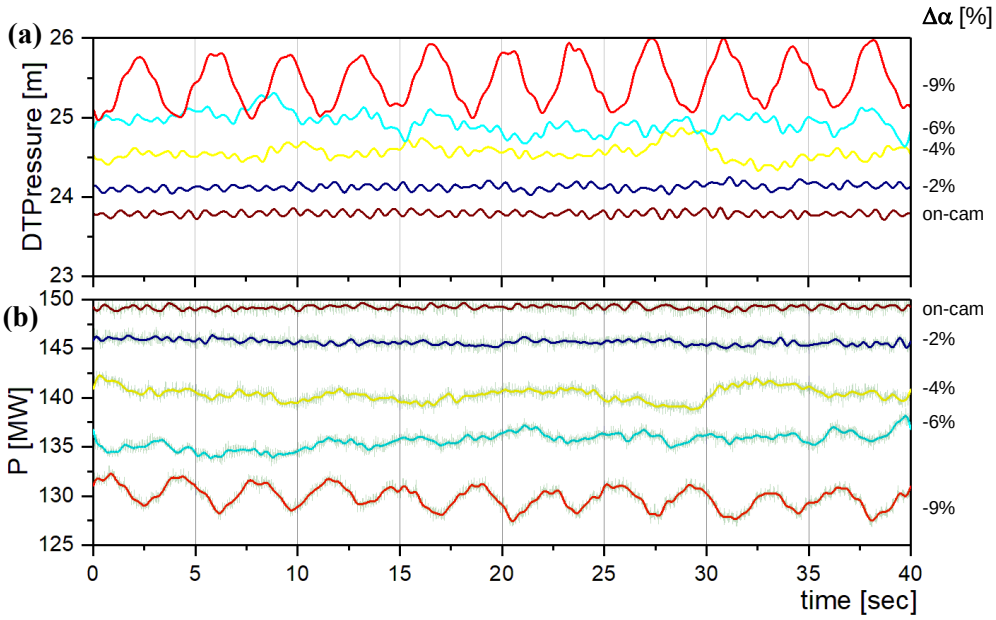

Figure 8. Filtered time signal of draft tube pressure for different guide vane positions (a). Filtered and raw time signal data for electrical power fluctuation for the same guide vane positions as above (b).

Figure 8. shows the evolution for both pressure at draft tube and generated electrical power signals from the on-cam position to Δα = -9%. For both signals a low pass filter with a cut frequency of 2 Hz, was implemented to have a cleaner signal. For on-cam to -2 % both signals stays without changes, but for lower values of Δα, the pressure and the power starts to disrupt increasing the amplitude but in a disordered way where no there is not a clear pattern or frequency, meaning that the partial load vortex rope it is not stable. For -9 % the amplitude is higher and the fluctuation frequency is clear. Therefore, the connection between the pressure at the draft tube and the power output can be proved.

If the pressure fluctuation is recalculated for the filtered signal it is possible to detect influence of vortex rope and an increase in pressure fluctuation can be seen when closing the guide vane, see figure 9.

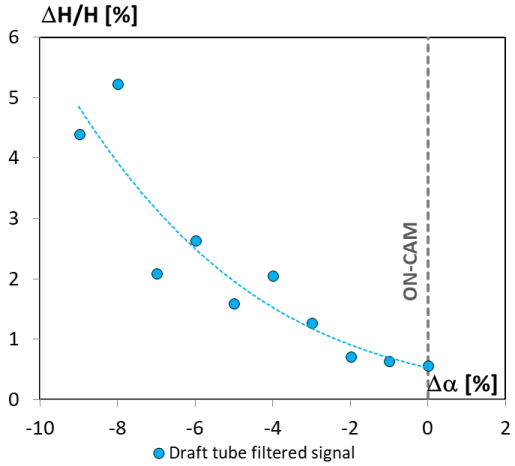

Figure 9. Pressure fluctuation for the filtered time signal for of draft tube pressure for different guide vane positions.

In order to capture the frequency of the vortex rope, a spectral analysis of the pressure and power signals is done by means of FFT. Figure 10. shows a clear rising tendency for the low frequency field. In both power and pressure spectra, a 0.231 f/fn peak frequency is detected at -9%. For higher Δα the peak for power is diffused, but for pressure starts a -8%. However, for the power fluctuation amplitude [figure 7 (a)] and for the physical model tests the rope starts at -8% also.

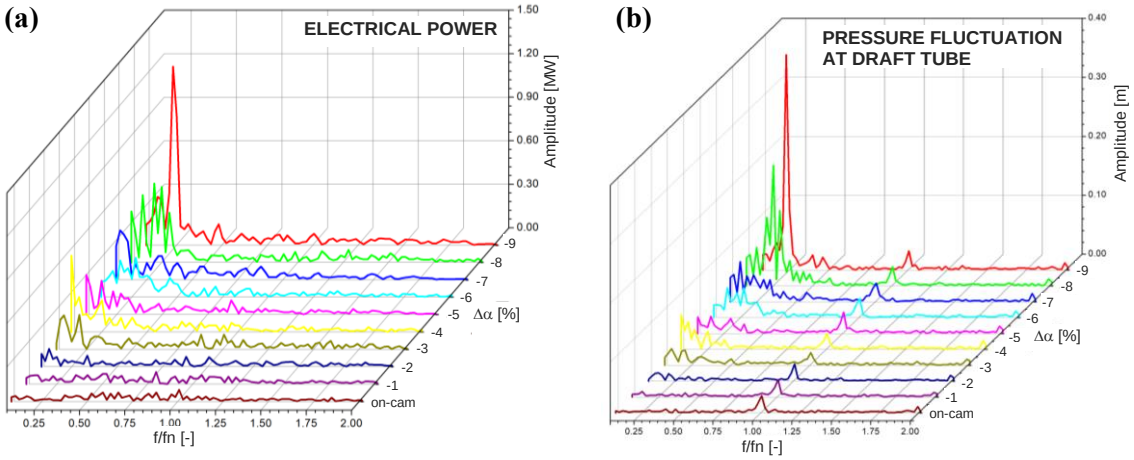

Figure 10. Waterfall spectra of electric power signals as Δα decrease (a). Waterfall spectra for the pressure signals at the draft tube (b).

3.2 CFD simulations

Transient results show the presence of the partial load rope visualized at physical model tests [2] and measured at prototype. The calculated frequency of the rope was 0.25 times the runner rotation frequency. From simulated point 1 to 4, the size of the rope increases, and the helical part of the rope moves upstream close to the runner. In table 3, results are summarized. When the guide vane close, pressure and power fluctuation increase due to the vortex development.

Figure 11. compare vortex rope visualization in physical model and CFD results. For point 2, although there is no cavitating vortex in the model, there is an incipient rope in the draft tube elbow that is detected in CFD using Q-criterion for vortex visualization.

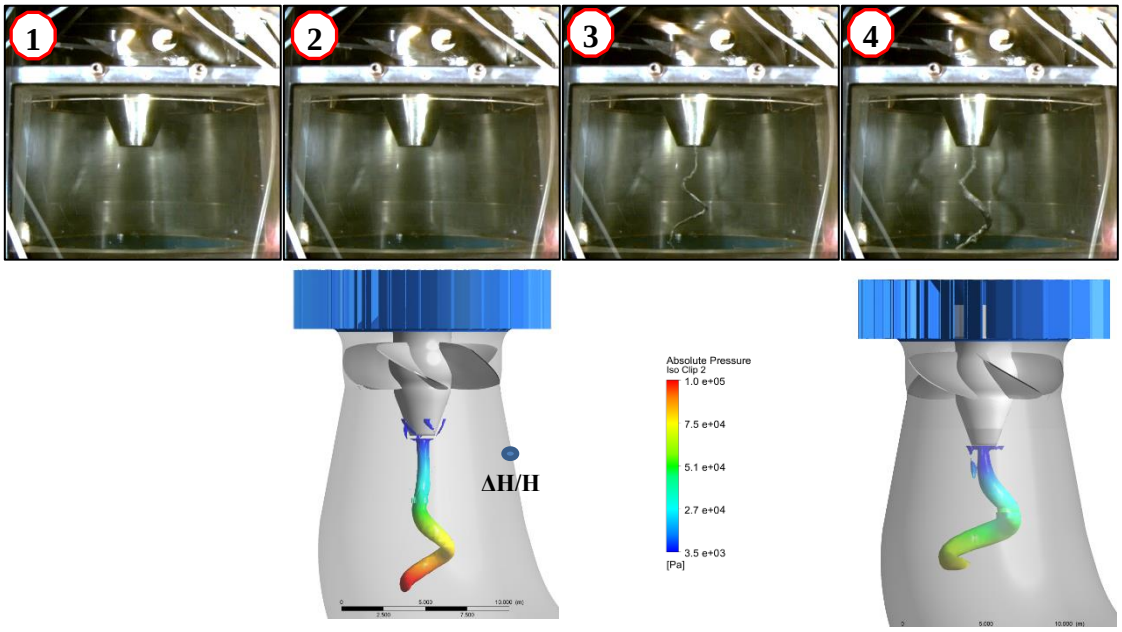

Figure 11. Physical model visualization of partial load rope (b) [2]. Vortex visualization applying the Q-criterion for off-cam condition corresponding to simulated point 2 and 4. For CFD simulations the vortex rope has a characteristic frequency at f/fn = 0.25.

Table 3. Pressure and mechanical power pulsation for CFD calculations and comparison with prototype measurements.

		CFD		Experimental	
Point	Δα [%]	Pressure ΔH/H [%]	Power Amp[MW]	Pressure ΔH/H [%]	Power Amp[MW]
1	0,0 (ON-CAM)	1,30	0,00	0,57	0,54
2	-2,8	2,10	0,00	1,27	1,56
3	-5,3	4,00	0,12	1,60	2,02
4	-7,9	5,30	0,18	5,23	3,47

4. Discussion and Conclusions

Prototype test were carried out on a Kaplan turbine working in propeller mode (with fixed blades). Accelerations at the draft tube and shaft guide bearing, pressure fluctuations, also sound measurements were done to characterize the machine behavior under off-cam operation until a partial vortex zone is reached. These measurements shown clearly that the most affected parameter is power fluctuation which can lead to power instabilities transmitted to electrical lines.

On the other side, CFD simulations were ran with the aim of capturing the power swing of the machine. Four guide vanes openings were simulated in a transient approach, to reproduce the on-cam and off-cam condition with a SST turbulence model and monophasic configuration for a time-step corresponding to 5 degrees of runner revolution, which thrown results in concordance with prototype measurements.

In terms of the flow field characteristics, CFD simulations effectively captured the shape of the partial load vortex rope and its characteristic frequency of 0.25 fn, which at prototype was 0.231 fn. More accurate frequency could be achieve decreasing the time step of calculation. Pressure and power fluctuation grow up to 5.3% and 0.18 MW for a $\Delta\alpha$ = -7.9%. Concerning to pressure fluctuations at draft tube, a good agreement between CFD results and the filtered signal from prototype measurements, see Table 3. CFD also could detect the guide vane opening where power generation starts to fluctuate due to partial load vortex.

However, power pulsation amplitude was underestimated comparing to prototype results. The reason for these differences could be related with two aspects: on one hand, prototype measurements contains several plant factors that are not considered at CFD model, on the other hand there is an interface between the stationary domain (draft tube) and the rotating frame (runner) that could be filtering the pressure fluctuations generated by vortex rope.

References

[1] U.S. Army Corps of Engineers 2009 *Kaplan turbine repair strategy*
[2] Angulo M, Rivetti A, Diaz L, Lucino C and Liscia S 2017 Kaplan turbine working as a propeller: methodology to redefine the operation zone *III IAHR Latin American hydro power and systems meeting (Quito)*
[3] International electrotechnical committee 1999 Hydraulic turbines, storage pumps and pump-turbines – model acceptance tests international standard IEC 60193, 2nd Edition
[4] Rivetti A, Angulo M, Lucino C and Liscia S 2015 Pressurized air injection in an axial hydro-turbine model for the mitigation of tip leakage cavitation *J. Phys.: Conf. Ser.* **656** 012069.
[5] Ruchonnet N, Nicolet C and Avellan F 2006 Hydro acoustic modelling of rotor stator interaction in Francis pump-turbine. *IAHR Int. Meeting of WG on Cavitation and Dynamic Problems in Hydraulic Machinery and Systems Barcelona 28-30*
[6] Nennemann B and Vu T C 2007 Kaplan turbine blade and discharge ring cavitation prediction using unsteady CFD. *Sci. Bull. Politehnica Univ. of Timisoara Transactions on Mech. **52(66)** no. 6*
[7] Franc J P, Avellan F and Kueny J L 1995 *La cavitation: mécanismes physiques et aspects industriels* Presses universitaires de Grenoble
[8] Rivetti A, Angulo M, Lucino C and Liscia S 2014 Mitigation of tip vortex cavitation by means of air injection on a Kaplan turbine scale model *IOP Conference Series: Earth and Environmental Science* **22** 52024.
[9] Rivetti A, Angulo M, Lucino C, Hene M, Capezio O, and Liscia S 2016 Implementation of pressurized air injection system in a Kaplan prototype for the reduction of vibration caused by tip vortex cavitation *IOP Conf. Ser.: Earth Environ. Sci.* **49** 022007.

Acknowledgement

The authors would like to thanks to the technical director of the Yacyretá power station, Eng. Marcelo Cardinali, and the personal of the regulation staff for their important contribution in prototype tests.